Contents lists available at SciVerse ScienceDirect

Energy and Buildings

Intermediate complexity model for Model Predictive Control of Integrated Room Automation

B. Lehmann [a,*], D. Gyalistras [b], M. Gwerder [c], K. Wirth [a,1], S. Carl [a]

[a] Empa, Swiss Federal Laboratories for Materials Science and Technology, Laboratory for Building Science and Technology, Ueberlandstrasse 129, CH-8600 Duebendorf, Switzerland
[b] ETH, Swiss Federal Institute of Technology, Automatic Control Laboratory, Physikstrasse 3, CH-8092 Zurich, Switzerland
[c] Siemens Switzerland Ltd., Building Technologies Division, Gubelstrasse 22, CH-6301 Zug, Switzerland

ARTICLE INFO

ABSTRACT

Integrated Room Automation (IRA) for office buildings deals with the automated control of blinds, electric lighting, heating, cooling, and ventilation of a room or building zone. Model Predictive Control (MPC) presents a promising method to achieve energy savings thanks to improved control. This paper presents the development and validation of an intermediate complexity, integrated building and building equipment model suitable for application within MPC. A resistance-capacitance (RC) modeling approach was chosen. The result is a 12th order multiple-input-multiple-output bilinear model for the coupled simulation of the thermal, light and air quality dynamics of a single room. It includes the subsystems mechanical and natural ventilation, radiator and floor heating, cooling ceiling and thermally activated building system. For computational efficiency and compatibility with MPC, several approximations and a reduction of complexity were necessary. The resulting behaviors were validated against detailed building and system simulations. The model was found to deliver accurate and reliable results. It can be flexibly configured to represent typical building types and variants of technical systems. Furthermore, it is sufficiently efficient to support large-scale sensitivity studies. Finally, the model is ready for adaptation and integration into commercial algorithms for the control of real buildings.

1. Introduction

The building sector accounts for a large portion of energy consumption and CO_2-emissions worldwide. For instance in Switzerland, approximately 45% of end energy is used for the operation of buildings i.e. for heating, air conditioning, domestic hot water and electrical appliances [1]. The pivotal question of building design therefore is to identify and exploit potentials for energy and CO_2 savings.

Modeling and simulation presents a powerful approach to explore the effect of alternative designs on energy usage and indoor comfort. The design variants will typically vary across three dimensions: the building construction (geometry, materials etc.), the building's technical equipment, and the way this equipment is operated, i.e. building control. The latter aspect becomes increasingly important with increasing system complexity, the use of intermittent energy sources (e.g. solar, wind), time-varying energy

prices, and slow building dynamics (e.g. due to the activation of the building's thermal mass).

The present study was motivated by the need to determine the control that yields the lowest possible energy usage for a given situation (building, location, utilization profile etc.) and set of comfort requirements. For the energy usage associated with this best possible control we use the term energetic performance bound (PB). By definition the PB presents a theoretical number that cannot be beaten by any real controller. Knowledge of a system's PB makes it possible to compare different design variants net of any effects related to control. A second implication is that any real controller's maximum possible improvement potential is given by the difference between its energy usage and the PB.

One possibility to estimate the PB – and the one addressed in this work – is to use so-called Model Predictive Control (MPC). MPC relies on the recurring application (for example, once every hour) of a mathematical optimization procedure. The latter takes into account the building's behavior based on a dynamic model. The optimization determines the sequence of control actions that minimizes a given cost function (e.g. the building's total energy usage) over a given prediction horizon (e.g. 1–2 days) while respecting some prescribed constraints such as the comfort range for room temperatures, the system dimensioning etc. The control actions identified for the very

* Corresponding author. Present address: Canton of Zurich, Building Department, Stampfenbachstrasse 12, CH-8090 Zurich, Switzerland. Tel.: +41 43 259 42 66; fax: +41 43 259 51 59.
E-mail address: Beat.Lehmann@bd.zh.ch (B. Lehmann).
[1] Permanent address: Kriesbachstrasse 15, CH-8600 Duebendorf, Switzerland.

Nomenclature

Variables, parameters, abbreviations

A	area [m^2]
α	opening angle windows [°]
C	heat capacity [J/(m^2 K)]
c_d	drag coefficient [–]
c_k	aperture factor window [–]
co_{CO_2}	CO_2-concentration outside [ppm]
cp	specific heat capacity [J/(kg K)]
cp_{CO_2}	CO_2 production persons [ppm]
cr_{CO_2}	CO_2-concentration room [ppm]
ERC	heat (energy) recovery ventilation
$Eroom$	room illuminance [lx]
$etaDl$	luminous efficacy daylight [lm/W]
$etaEl$	luminous efficacy electrical lighting [lm/W]
ε	thermal efficiency ERC, free cooling efficiency [–]
η	(room) utilance [–]
g	acceleration of gravity [m/s^2]
H	height [m]
h	heat transfer coefficient [W/(m^2 K)]
k	abbreviation [m^3/s]
IRA	Integrated Room Automation
$mevGe$	heat gain ventilation with ERC [Wh/m^2]
$mevG0$	heat gain ventilation without ERC [Wh/m^2]
MPC	model predictive control
No	number of
$nNav$	air change rate natural ventilation [h^{-1}]
oW	outer walls
PB	performance bound
$\dot{q}$	heat flux [W/m^2]
RBC	rule based control
RC	resistance capacitance (network)
sa	swiss average insulation level
st	swiss target insulation level
T	temperature [°C]
$TABS$	thermally activated building system
τ	(solar, visual) transmittance [–]
ϑ	temperature [°C]
Mev, mev	mechanical ventilation
pa	passive house insulation level
R	thermal resistance [(m^2 K)/W]
RG	incident global solar radiation [W/m^2]
RGS	global solar radiation component on south facing vertical wall [W/m^2]
U	heat transmission coefficient [W/(m^2 K)]
V	volume [m^3]
$\dot{V}$	air flow rate [m^3/s]
W	width [m]

Subscripts

0, 1, 2 . . .	index
A, air	air
bl	blind
$bl0$	blind, fully closed
$Ceil$	ceiling
$Comb$	combined
Cov	cover, e.g. carpet
ct	cooling tower
dl	daylight
el	electrical
$Floor$	floor
gl	glazing
i	index

in	inlet
inf	infiltration
Ins	insulation
iW	inner walls
max	maximum
mev	mechanical ventilation
min	minimum
nav	natural ventilation
oW	outer walls
r	room
$s, slab$	slab
sp	set point
sw	supply water
t	total
SS	single sided natural ventilation
vis	visual
win	window

Control inputs

$bPos$	blind position [0: closed. 1: open] [–]
$eLighting$	gains electric lighting [W/m^2]
$hPowSlab$	heating power slab [W/m^2]
$cPowSlab$	cooling power slab [W/m^2]
$fcUsgFact$	free cooling usage factor [–]
$nMevE$	air change rate mech. vent. with ERC [1/h]
$nMev0$	air change rate mech. vent. without ERC [1/h]
$hPowMev$	heating power (mev), positive values = heating [W/m^2]
$cPowMev$	cooling power (mev), positive values = cooling [W/m^2]
$nNav$	air change rate natural ventilation [1/h]
$hPowRad$	heating power (radiator) [W/m^2]

Disturbance inputs

$Tair$	outside air temperature [°C]
$Tfresh$	fresh air temperature mech. ventilation [°C]
$TfreeCool$	free cooling temperature [°C]
$solG$	solar gains with fully closed blinds [W/m^2]
$dSolG$	additional solar gains with open blinds [W/m^2]
$illum$	daylight illuminance with fully closed blinds [lux]
$dillum$	additional daylight illuminance with open blinds [lux]
$persG$	internal gains (persons) [W/m^2]
$equipG$	internal gains (equipment) [W/m^2]
$nInf$	air change rate infiltration [1/h]

first time step within the prediction horizon are then applied to the system, and the whole procedure is repeated at the next time step.

A given design variant's PB can be estimated applying MPC over a representative period (e.g. one year) assuming a perfect building model, and perfect knowledge of all future disturbances (weather, internal gains etc.). Clearly, when MPC is used for real control, its performance will critically depend on the extent to which the used building model matches the real system; on the data available for initializing the model at begin of each optimization, and on the accuracy of the disturbances predictions.

In the framework of the research project OptiControl on the use of weather and occupancy forecast for optimal building climate control (www.opticontrol.ethz.ch) we were interested in systematically analyzing the PB and optimization potentials of state-of-the-art controllers for the application Integrated Room Automation (IRA). IRA is dealing with the combined control of heating, cooling, ventilation, blinds and lighting in buildings.

Initial investigations showed that the PB and the controller improvement potentials varied widely between design variants, controllers, sites etc. This implied the need for a configurable, easy to parameterize, and flexible model that could be used to investigate a large variety of cases by means of systematic simulation studies. Moreover, the model had to be as simple as possible to minimize the computational effort for the optimization involved in MPC. On the other hand it had to be sufficiently detailed to accurately represent the relevant physics of the modeled processes. Finally it was required that the model could be used as both, as a controller model for MPC, and as a plant model for the assessment of the different controllers.

Here we report on the development of such a novel, MPC-compatible building and building equipment model that satisfies the above requirements. The objectives of this article are to:

- Provide rationale for the chosen modeling approach including the necessary approximations;
- Describe how the buildings and building systems for the IRA control task were modeled, and to provide a mathematical description where appropriate;
- Validate the various involved sub-models, giving information on their accuracy, validity range and applicability restrictions, and
- Draw conclusions concerning the applicability of the model within large scale simulation studies as well as within real world building automation control systems.

2. Choice of modeling approach

The choice of modeling approach was based on the following profile of requirements:

- The resulting model should be detailed enough to provide a reliable simulation of the building's dynamics and of all control relevant processes. To this end it was considered necessary to model walls, floors and ceilings using at least three layers, and to use a temporal resolution of 1 h or less.
- The model should be simple enough to be incorporated in an MPC controller. Moreover, the MPC should not require too much computational effort. This implied restricting the optimization task to so-called linear or quadratic programs for which efficient numerical solvers are available. This in turn imposed the restriction of having to use a linear or at most bilinear representation of the system dynamics.
- The model should be suitable for large-scale simulation studies aiming at the systematic investigation of different building configurations, building sites, comfort requirements etc. The model therefore should be computationally efficient, have reasonable input data needs and be flexibly customizable to support several representative building types and common building equipment.

Modeling of buildings has a long history such that many different models of varying complexity and purposes have been developed so far.

The most sophisticated models available are whole building energy simulation programs like EnergyPlus [2], ESP-r [3], IDA ICE [4] or TRNSYS [5]. They support detailed and realistic modeling of a huge range of building features, the modular integration of technical system simulation modules, and variable time steps. However, they employ highly non-linear physics and have extensive input data needs. Hence they are far too complex for being considered in a model predictive controller, and moreover their execution times can become prohibitive for large-scale simulation studies.

Therefore we resorted to using a much simpler description of the building's thermal dynamics based on a thermal resistance-capacitance (RC) network. A well-known model from this class is the RC model used in standard EN ISO 13790 [6]. It comes with a method to approximate the thermal behavior of multizone buildings with three thermal nodes and one heat capacitance. Although the model allows for the calculation of the hourly heating and cooling energy demand its accuracy at the hourly time scale is strongly limited by the use of a lumped thermal mass, and by the simplified consideration of building systems based but on mean characteristics and efficiencies. More sophisticated RC models have already been developed for MPC in the context of mechanical and natural ventilation systems [7,8], floor heating [9], various heating and cooling systems [10,11] or active and passive thermal energy storage systems [12,13]. A number of studies like [14] have also dealt with the combined optimization of thermal comfort and energy consumption in buildings.

However, for several reasons none of the existing models proved suitable for the intended purposes: (i) typically the focus was but on a single building system or application only, whereas we were interested to support a wide range of equipment. (ii) The solutions were typically tailored to one specific building and therefore offered too little flexibility to represent differing building constructions and configurations. (iii) For MPC was mostly used a simplified modeling of the building structure in the form of lumped thermal masses such that the thermal behavior of individual rooms was not represented accurately enough.

To keep the newly developed model as simple, flexible and modular as possible we chose to focus on a single building zone. This approach was motivated by the fact that key features (e.g. energy consumption) of whole buildings can be reproduced reasonably well by summing up or extrapolating the results obtained for different characteristic rooms of the building. These rooms will typically either differ in terms of construction and/or thermal gain situation. The main application area for IRA is office buildings which often show a consistent occupancy pattern. Hence individual rooms will typically differ mainly in terms of the number and the orientation of façades, and this variation can be well captured by a single zone model.

3. Model variants

In terms of the building construction the zone/room was defined by the following set of attributes: façade orientation, construction type, building standard, and window area fraction of the façade.

Fig. 1 shows two selected configurations as an example, and Table 1 gives an overview of the attribute values considered.

The choice of values sets for the various attributes (Table 1) presented a compromise between two conflicting objectives: on the one hand we aimed at covering as many realistic situations as possible, on the other hand we had to keep the total number of cases (as given by all possible combinations of attribute values) sufficiently small in order to restrict the needed overall computational effort for a systematic investigation.

The solution to the IRA control task clearly depends strongly on the building system at disposal. Many such systems occur in practice.

For this study we considered five typical variants of building systems that employed different combinations of automated subsystems (Table 2).

As can be seen from Table 2 all five systems included automated blinds and light control. For system variants S2–S5, which all involve mechanical ventilation, we also assumed the presence of a subsystem for energy recovery from the facility's exhaust air stream.
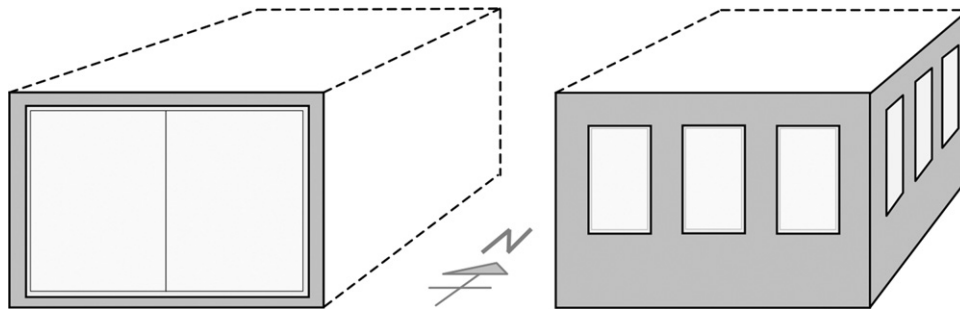
Fig. 1. Schematic representation of two building zones. Left: normal office, façade orientation "South" (S), window area fraction "high" (80%); right: corner office, façade orientations "South + East" (SE), window area fraction "low" (30%).

Table 1
Considered building attributes and associated sets of attribute values.

Attribute	Value	Identifier	Remarks[a]	
Façade orientation	North	N	Middle office	
	South	S	Middle office	
	South + East	SE	Corner office	
	South + West	SW	Corner office	
Construction type	Heavyweight	h	$c_{dyn} \approx 80\,\text{Wh/m}^2\,\text{K}$[b]	
	Lightweight	l	$c_{dyn} \approx 36\,\text{Wh/m}^2\,\text{K}$	
Building standard	Swiss average	sa	$U_{op} \approx 0.6\,\text{W/m}^2\,\text{K}$[c]	$U_{win} = 2.8\,\text{W/m}^2\,\text{K}$[d]
	Passive house	pa	$U_{op} \approx 0.1\,\text{W/m}^2\,\text{K}$	$U_{win} = 0.7\,\text{W/m}^2\,\text{K}$
Window area fraction	Low	wl	30% window area	
	High	wh	per façade	
			80% –	

[a] Reference for c_{dyn} and U-values is the floor area.
[b] c_{dyn}: internal dynamic heat capacity of the room.
[c] U_{op}: overall heat transfer coefficient of opaque façade parts.
[d] U_{win}: overall heat transfer coefficient of windows including frame.

Table 2
Building systems considered. "x" denotes the presence of a subsystem and the variables in brackets are the associated control inputs.

| Automated subsystems	Building system				
	S1	S2	S3	S4	S5
Blinds (*bPos*)	x	x	x	x	x
Electric lighting (*eLighting*)	x	x	x	x	x
Mechanical ventilation with heating, cooling and energy recovery (*nMev0, hPowMev, cPowMev, nMevE*)	–	x	x	x	x
Natural ventilation heating/cooling (night-time only) (*nNav*)	–	–	–	x	–
Cooling ceiling (capillary tube system) acting through cooling ceiling or TABS (*cPowSlab*)	x	x	–	–	–
Free cooling with wet cooling tower (*fcUsgFact*)	x	x	–	–	x
Radiator heating (*hPowRad*)	x	x	–	–	–
Floor heating (*hPowSlab*)	–	–	–	x	–
Thermally activated building systems (TABS) for heating/cooling (*hPowSlab*), (*cPowSlab*)	–	–	–	–	x

System variant S1 was the only one with no ventilation subsystem present. System variant S2 had the same heating and cooling subsystems as variant S1, but in addition also a mechanical ventilation subsystem. Variant S3 was defined to have only a ventilation subsystem, i.e. no other subsystems were assumed to be at disposal for heating and cooling. Finally, system variants S4 and S5 were introduced to investigate hybrid (mechanical + natural) ventilation schemes, and the use of Thermally Activated Building Systems (TABS), respectively.

4. Model description and validation

4.1. Overview

Figs. 2 and 3 give an overview of the model's components and the RC-network, respectively.

The model is constructed around the central room node ϑ_r. The massive structure of the building consists of a combined floor/ceiling slab, a façade wall with integrated windows and an internal wall. The floor, the ceiling and the interior wall demarcate
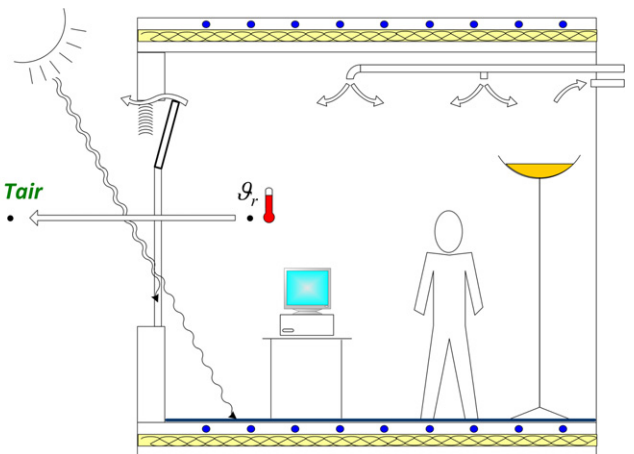
Fig. 2. Schematic representation of the model using the example of the building equipped with system variant S4 with floor heating and natural ventilation.
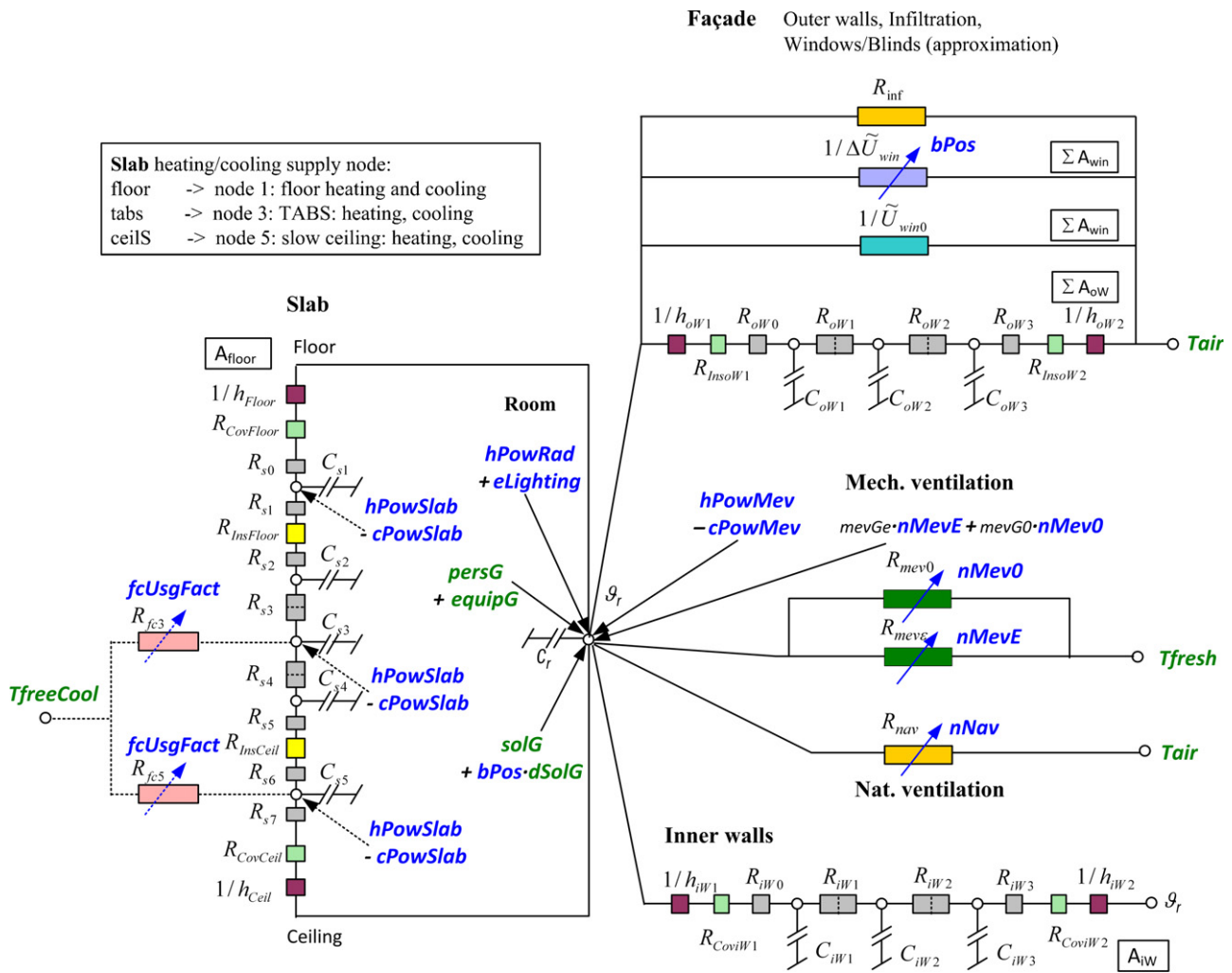
Fig. 3. Thermal Resistance-Capacitance (RC) network model. Note that for illustration all supported subsystems are shown simultaneously. For explanation of identifiers see Nomenclature.

the room from the neighboring rooms. These rooms are assumed to have identical temperature dynamics (ϑ_r) and boundary conditions as the room modeled. This translates into the assumption that this room is not influenced by neighboring rooms, i.e. it is one in a large series of identical (in terms of heat fluxes) rooms located vertically and horizontally relative to it.

The structural elements were represented by the following numbers of nodes: floor/ceiling 5 nodes, and façade and internal wall 3 nodes each. These numbers were chosen such as to enable the correct representation of heat fluxes from the technical systems into the floor/ceiling, and to provide sufficient resolution for the simulation of heat storage and of heat transfer through the walls.

The various heating and cooling system heat fluxes apply either to the room node or – depending on the chosen slab system – on one of the slab nodes (floor heating: node 1, when counting from top to bottom; TABS: node 3; cooled ceiling: node 5). Internal gains from persons, equipment and lighting as well as solar gains are transferred entirely to the room node.

4.2. Thermal mass, room heat exchange and solar gains (thermal building model)

The RC-modeling approach and the used simplifications affected the representation of various physical mechanisms that

determine the thermal behavior of a room in a real building: the long wave radiation exchange between building envelope and sky was neglected, as this was done for the solar absorptance of opaque external surfaces; the combination of different wall surfaces to lumped walls lead to a simplified representation of the internal long wave radiation exchange within the room; modeling of the windows employed approximations for the transmittance of solar radiation; and finally heat transfer through the walls was approximated by representing them using a minimum possible number of thermal nodes (cf. Fig. 3).

To assess the effect of these simplifications we tested the proposed model against a physically detailed reference model that was based on the well-known building simulation software TRNSYS [5]. To verify the relative importance of the various assumptions we simplified the TRNSYS model step by step until we arrived at a model that corresponded to the proposed RC modeling approach. Starting from the full-scale reference model its complexity was reduced in four steps:

Step 1: Long wave radiation exchange with the sky was simplified by using combined heat transfer coefficients for convection and radiation and assuming the sky temperature to be equal to the outside air temperature; solar absorptance of opaque walls was neglected; usage of lumped instead of individual walls.
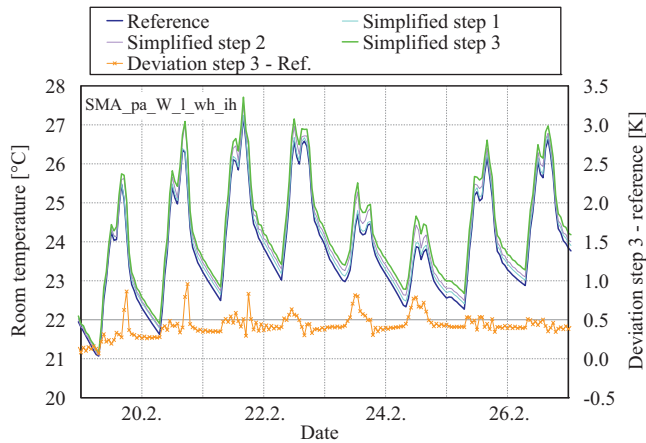
Fig. 4. Effect of successive model simplification on room temperature dynamics.

Fig. 5. Errors due to the linearization of the heat transfer through windows and blinds.

Step 2: Introduction of simplified heat exchange within the room, using combined heat transfer coefficients for convection and radiation.

Step 3: Simplified model for heat conduction and solar transmission of windows.

Step 4: Simplified heat transfer through walls by use of a limited number of thermal nodes.

To avoid modeling of control actions the simulations were compared for a free floating phase of the building where the room temperature varied within the assumed comfort bounds without active heating or cooling. The advantage of this approach was that it allowed us to validate only the thermal dynamics of the building, i.e. the comparisons were not distorted by any differences in building equipment sub-models.

Fig. 4 exemplarily compares the room temperatures simulated by the TRNSYS reference model to the simplified TRNSYS models from the first three simplification steps and for the building configuration "SMA_pa_W_l_wh_ih", where SMA refers to the use of weather data from site Zurich (for a description of the remaining identifiers used to compose the case name see Table 1). It can be seen that the average deviation obtained for the model involving all simplifications up to Step 3 as compared to the reference model was in the order of +0.5 K (with single peaks up to 1.0 K). If the general drift of this case was eliminated (as would be the case under controlled operation), the remaining maximum relative deviation would reduce to −0.2/+0.5 K.

The simplified (up to step 3) TRNSYS model differed from the proposed RC model but in one essential point, the implementation of the walls and the slabs. In TRNSYS the heat transfer through massive walls and slabs is modeled with the aid of an accurate response factor method. In contrast, each wall within our much simpler RC model was represented by a fixed RC-configuration (cf. Fig. 3).

The impact of this remaining model difference (Step 4) was evaluated by a direct comparison of the RC model and TRNSYS results. To this purpose the disturbances and selected control inputs as precalculated in the RC model run were fed into TRNSYS. It was found that the RC modeling errors were in the order of −0.2/+0.4 K (results not shown).

A simple summation of the found maximal deviations from all model simplifications (Steps 1–3 after drift removal, plus Step 4) yields maximum deviations of −0.4/+0.9 K. Since the deviations of the individual simplifications do not occur simultaneously or may even cancel each other out, considerably smaller deviations can be expected to occur during most of the time.

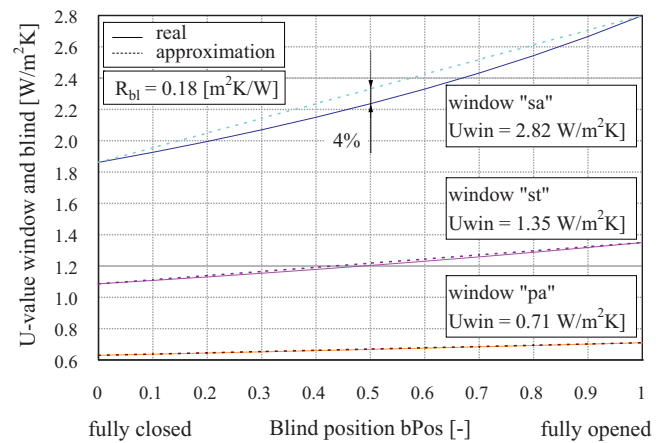Though not negligible, these remaining deviations are small when compared to expected output uncertainties of common building simulation codes. Therefore it can be concluded that the proposed 12th-order RC-model allows for a realistic representation of the investigated building zone's thermal dynamics. Moreover, note that the investigated case presents a rather extreme case compared to the building thermal characteristics found in the current building stock (light weight building with high window area fraction and high internal gains). Hence we believe that our conclusion also holds for many other building configurations as well.

4.3. Windows and blinds modeling

In IRA, the light level in the room, the solar gains, and the convective heat transfer through the windows are controlled by means of external blinds. Their position can be continuously varied between fully opened ($bPos = 1$) and fully closed ($bPos = 0$).

The radiative heat flux through the windows was modeled by adjusting the maximum possible heat flux as given by the window's solar heat transmittance factor as a linear function of blind position.

The heat transfer through the windows and the blinds follows a non-linear characteristic (cf. Eq. (1)).

$$U_{comb} = \frac{1}{R_{win} + (1 - bPos) \cdot R_{bl}} \tag{1}$$

To meet the requirements according to Section 2, this characteristic was linearized between the two extreme cases of fully closed ($\tilde{U}_{win0}$) and fully opened blinds ($\tilde{U}_{win}$) based on the following approximation (Eq. (2)).

$$\tilde{U}_{win0} = \frac{1}{R_{win} + R_{bl}}; \quad \tilde{U}_{win} = \frac{1}{R_{win}}$$
$$\Delta\tilde{U}_{win} = \tilde{U}_{win} - \tilde{U}_{win0} \tag{2}$$
$$\tilde{U}_{comb} = \tilde{U}_{win0} + bPos \cdot \Delta\tilde{U}_{win}$$

Fig. 5 shows the errors due to the linearization for the various used blind and window types. As can be seen, the errors were generally small. They reached a maximum of 4% in the case of the "Swiss average" window and diminished with decreasing U-value of the window. We concluded that owing to the small inaccuracies the proposed approximation is applicable without constraints.

4.4. Mechanical ventilation

To enable consideration of typical systems found in office buildings and to explore the automated regulation of indoor air quality a mechanical ventilation system was implemented in the model (Fig. 6). It included energy recovery (contribution to the room's air change rate: nMevE) e.g. with a rotary or a counter current heat
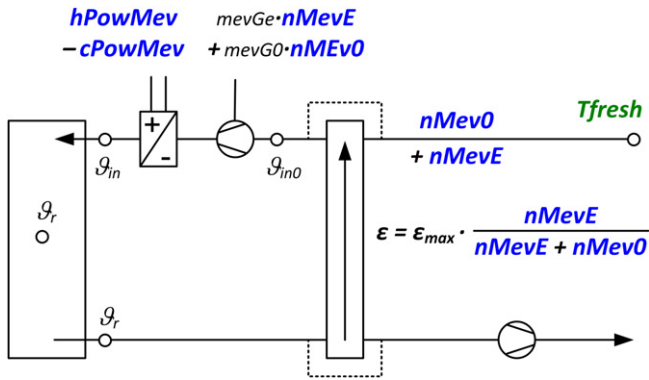
Fig. 6. Mechanical ventilation model with energy recovery, heating and cooling.

exchanger (efficiency $\varepsilon = 0.8$), a bypass (air change rate $nMev0$) as well as heating and cooling coils (heating and cooling power $hPowMev$ and $cPowMev$, respectively) for the conditioning of the supply air. Finally, the dissipation of energy into the air stream by the ventilators was also considered (heat gains $mevGe$ and $mevG0$ with and without ventilation, respectively).

Standard EN 15251 [15] stipulates that indoor air quality in common office rooms should meet at least comfort category II. Accordingly, the maximum threshold of the CO_2-concentration in the room was fixed at 900 ppm.

For control we considered the following two widespread ventilation strategies: *VS*1: non-air-quality-controlled ventilation with a constant air flow rate. Ventilation was assumed to operate only on working days from 06:00 to 19:00, using a constant air change rate design value as determined for maximum occupancy. *VS*2: CO_2-controlled ventilation. Here the air change rate was assumed to be controlled depending on the occupancy density. This control was not modeled explicitly, but was instead approximated by varying the air change rate with occupancy density. The rationale for this approximation and the validation of the approach are given in Section 4.4.1.

To ensure occupant comfort the ventilation inlet air temperature was assumed to be limited to minimum and maximum values of 16 °C and 40 °C respectively. As the thermal balance for the supply air temperature could not be modeled by a bilinear function we had to develop an approximation. It is explained in Section 4.4.2.

4.4.1. Approximation for CO_2-controlled ventilation mode

The CO_2-concentration in a room in reality shows very fast dynamics and depends on the production by persons and the exchange with outside air through infiltration and ventilation. To explicitly simulate these dynamics it would have been necessary to employ a time step in the order of 5 min or less. Given that the used time horizon for MPC was typically at least one day, this would

have resulted in a prohibitive increase of the needed computation time for the optimizations. Instead, CO_2-control was approximated by computing the air change rate as a linear function of occupancy density. Indoor air quality (CO_2-concentration in the room) was thus not controlled directly, but followed from the chosen strategy and air supply parameters.

Simulation results were analyzed to verify whether this approach allowed to satisfy the posed comfort requirements. As can be seen from a typical example as shown in Fig. 7, ventilation strategy *VS2* complied with comfort class II, but never exploited the fully possible concentration limit of 900 ppm. The chosen approximation of CO_2-control therefore yielded a somewhat higher air change rate (and hence energy usage) than would have been possible using explicit control at the <5 min time scale.

For comparison Fig. 7 also displays the results for the non-air quality controlled ventilation strategy (*VS*1). Because a constant air flow rate is used regardless of the actual occupancy, an even better comfort level was typically reached, and therefore this control strategy complied most of the time with the highest comfort class (class I, concentration limit of 750 ppm).

4.4.2. Approximation for ventilation supply air temperature limits

As apparent from Eq. (3), the thermal balance for the inlet air temperature is a nonlinear function of the air change rates $nMevE$ and $nMev0$.

$$\vartheta_{in} = Tfresh + \frac{nMevE}{nMevE + nMev0} \cdot \varepsilon_{\max} \cdot (\vartheta_r - Tfresh)$$

$$+ \frac{hPowMev - cPowMev + nMevE \cdot mevGe + nMev0 \cdot mevG0}{C_r(nMevE + nMev0)} \quad (3)$$

This function did not fit the needed bilinear framework, such that the allowed 16–40 °C range for the ventilation supply air temperature could not be specified directly. Instead, it was enforced by introducing constraints to the power of the heating and cooling coils used to condition the supply air. Details can be found in [20, Appendix A]. The approach was tested for selected representative building cases. It was found that the allowed temperature range was not fully exploited such that the used approximation can be considered to be on the safe side.

4.5. Natural ventilation

Building system S4 was defined such that it uses a combination of mechanical ventilation during occupancy hours and natural ventilation by window opening for night-time cooling. To make our model generally applicable we assumed single sided window opening because in this case the associated air flow is independent of the pressure distribution in the rest of the building. It was assumed that 4 bottom hung windows with dimensions of width $W = 1.0$ m and
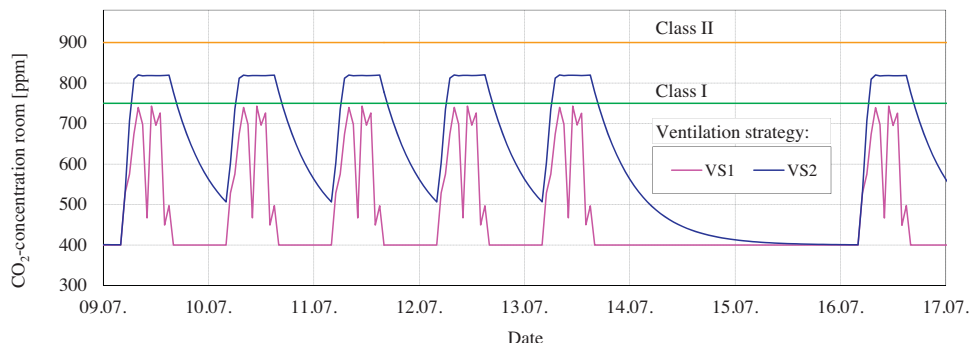

Fig. 7. Simulated CO_2-concentrations in office rooms depending on the applied ventilation strategy.
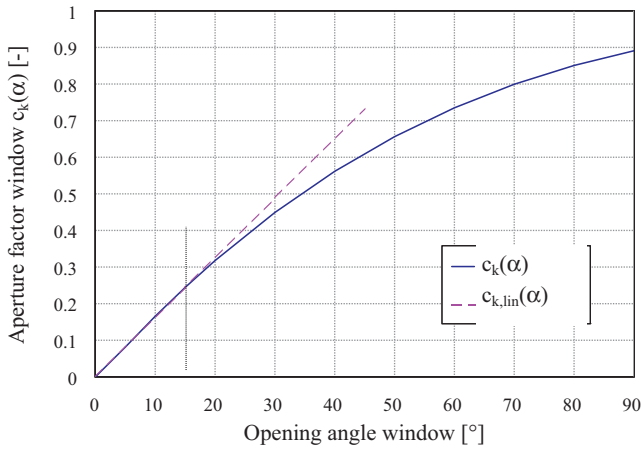
Fig. 8. Aperture factor $c_k(\alpha)$ for the air flow rate through bottom hung windows.

Fig. 10. Detail period night time cooling potential: heat transfer compensated (27.7), underestimated (28.7) and overestimated (31.7).

height $H = 1.4$ m can be opened up to a maximum opening angle of $\alpha = 15°$. This corresponded to the opening of all windows for cases with low window area fraction (wl) and was also applied for cases with higher fractions (where windows were assumed to be opened only partially to achieve the same maximum aperture state).

Natural ventilation was modeled using a physical correlation for the thermally driven air flow rate through windows ([16] and Eq. (4)). Eqs. (5) and (6) show the correlations for the resulting natural air change rate n_{Nav} in the room as well as the corresponding heat flux $\dot{q}_{Nav}$. It can be seen that the heat flux is a nonlinear function of the difference between outside air and room temperature. To achieve a bilinear formulation n_{Nav} had to be linearized. This was done by using a linear approximation for the aperture factor $c_k(\alpha)$ and by choosing a constant working point for the remaining terms, as follows: first, as stated above, the maximum allowed window opening angle was set to $\alpha = 15°$ since up to ca. $20°$ $c_k(\alpha)$ depends linearly on the angle (Fig. 8). Second, the temperature dependency under the square root in Eq. (5) was approximated by a constant value. The following criteria were considered to choose a suitable working point: (i) the night time cooling effect should be modeled most accurately when it is most critical, i.e. when room and outside air temperature differ only by a small amount (typically during warm summer nights); (ii) very high air change rates should be avoided to prevent undercooling of the room.

As shown in Fig. 9 an acceptable agreement between the linearized and the non-linear model for the natural ventilation heat
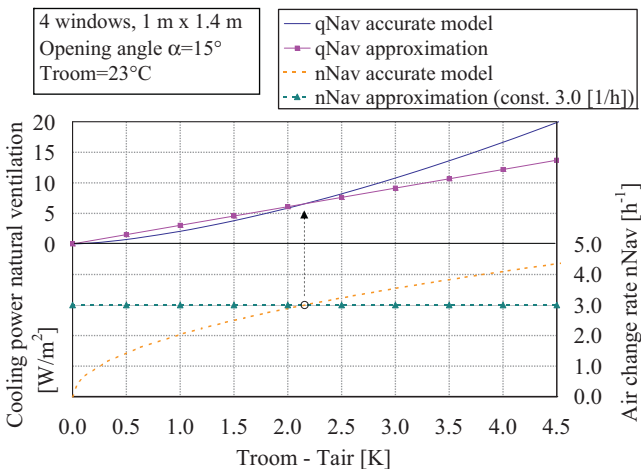
flux can be reached at a temperature difference of 2.2 K. For the maximum opening angle of $15°$ this corresponds to an air change rate of $n_{Nav_{max}} = 3.0$. Regardless of the actual temperature difference, the maximum air change rate by natural ventilation in the model was limited to between 0 and 3.0 [h^{-1}]. The control input n_{Nav} thus implicitly defined the opening angle of the window.

$$\dot{V}_{SS} = c_k(\alpha) \cdot c_d \cdot W \cdot H \cdot \frac{1}{3}\sqrt{g \cdot H} \cdot \sqrt{\frac{|Tair - \vartheta_r|}{Tair + 273}} \tag{4}$$

(1 bottom hung window)

$$nNav = \dot{V}_{SS} \cdot \frac{No_{win}}{V_r} = c_k(\alpha) \cdot k \cdot \sqrt{\frac{|Tair - \vartheta_r|}{Tair + 273}} \cdot \frac{No_{win}}{V_r} \tag{5}$$

(No_{win} bottom hung windows)

where $k = c_d \cdot W \cdot H \cdot \frac{1}{3}\sqrt{g \cdot H}$

$$\dot{q}_{Nav} = nNav \cdot \frac{V_r}{A_r} \cdot \rho_a \cdot cp_a \cdot (Tair - \vartheta_r) = c_k(\alpha) \cdot k \cdot \sqrt{\frac{|Tair - \vartheta_r|}{Tair + 273}}$$
$$\cdot \frac{No_{win}}{A_r} \rho_a \cdot cp_a \cdot (Tair - \vartheta_r) \tag{6}$$

As the temperature difference typically increases throughout the night the deviations of the linearized model from the theoretical curve can be expected to cancel out during the opening time of the windows. To quantify this effect we used MPC-derived profiles of window opening angles and times and compared the approximated cooling energy with the corresponding theoretical cooling potential. To this end we considered a total of seven annual simulations for different building types at the sites SMA and LUG. Selected, typical results are shown in Fig. 10. Our analyses (details not shown) showed that:

- Low air change rates (and the associated energy fluxes/cooling potentials) are modeled with reasonable accuracy.
- The simplified model only very rarely overestimates the air change rate over an entire night. This means that in reality the calculated approximative energy transfer can be achieved in most cases, even during summer nights.
- The simplified model considerably underestimates the achievable overall air change rates during many nights, with whole-night cooling energy fluxes being underestimated by 20–60%. The largest deviations were found to occur during hours

Fig. 9. Approximation of natural ventilation by a constant maximum air change rate of $n_{Nav_{max}} = 3.0$ h^{-1} and resulting cooling power errors.
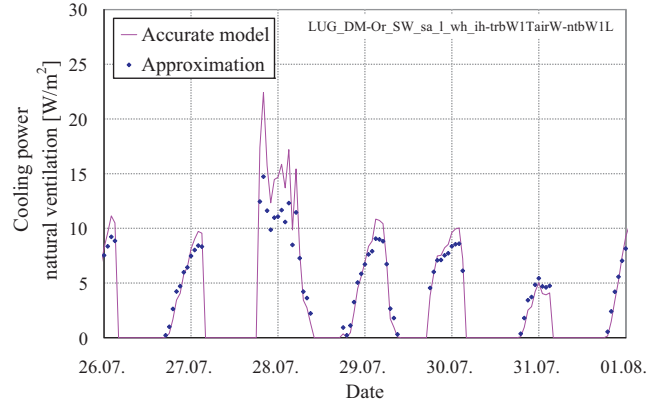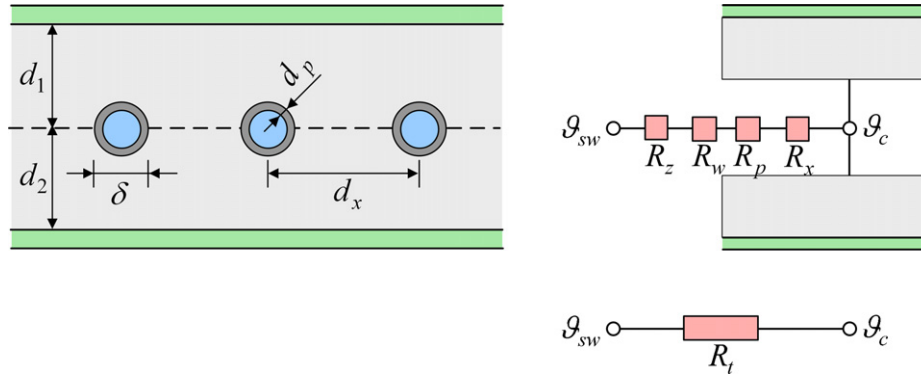
Fig. 11. Dynamic model for the heat transfer of slab embedded piping systems.
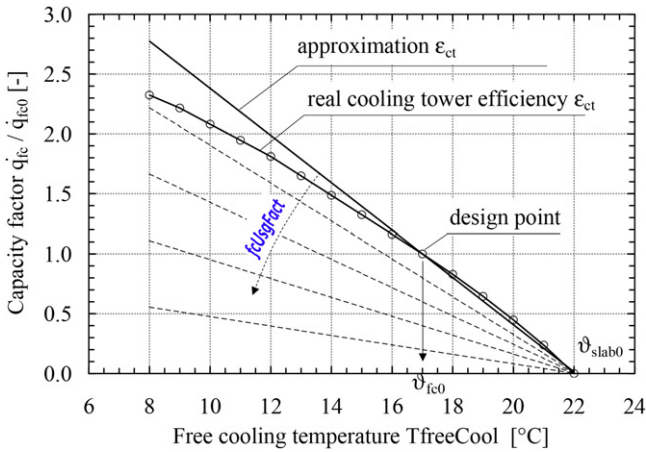

Fig. 12. Typical characteristic and design of a wet cooling tower used for TABS.

that showed a large difference between room and outside air temperature. This means that for mid-latitude sites the model will be typically most accurate during summer nights (when temperature differences are in the order of a few K) and less reliable during spring and autumn.

The bias toward an underestimation of air change rates/cooling potentials translates in the PB calculations to a somewhat increased usage of other (more energy intensive) cooling sources, and thus to somewhat inflated PB values. Regarding the use of the proposed model in a real application note that MPC would normally not be used to control the opening of the windows directly, but rather to compute an "optimal" room temperature setpoint for the next, say, 15–30 min. This setpoint would then be tracked by a much faster low-level controller. The under- or overestimation of air change rates by the MPC model would thus translate into somewhat suboptimal room temperature setpoints, but otherwise the low-level controller would protect the room from undercooling, or, if specified so by the setpoint, it could provide additional cooling by prolonged opening of the windows.

4.6. Slab systems cooling ceiling and TABS

Slab systems like cooling ceilings and TABS use a slab-embedded piping system to activate the thermal mass of the building structure and use it as a heat or cold storage. Because by design a considerable part of the system power is transferred directly to the building mass the heat or cold is released only with delay to the room.

The representation of heat transfer in slab-embedded piping systems in our model was based on the work by Koschenz et al. [17,18]. Their model uses a system characteristic R_t that serves reducing the 3-dimensional heat transfer within the slab to a linear, 1-dimensional correlation for the heat transfer between the supply water and the slab at the piping system's location (cf. Fig. 11). The correlation considers the supply water temperature and the mean core temperature (Eq. (7)). It has been tested thoroughly and it was shown to deliver accurate results for typical designs (geometry and mass flow rates) of TABS and surface mounted cooling ceilings found in practice [17].

The model by Koschenz et al. is mainly applied in conjunction with free cooling. There the supply water temperature depends on the actual free cooling conditions (cf. Section 4.7). For other generation systems like mechanical cooling and also for heating we assumed that – provided a proper system design – the required supply water temperatures can be achieved at any time. In these cases heating and cooling power (*hPowSlab*, cPowSlab) are directly fed into the slab node where the piping system is located.

$$\dot{q} = \frac{1}{R_t} \cdot (T_{sw} - T_{slab}) \tag{7}$$

4.7. Free cooling with wet cooling tower

Free cooling with a wet cooling tower was modeled using an overall system correlation R_{fc} that was developed in the framework of a research project on the modeling of TABS [17]. The correlation describes the heat transfer all the way from the free cooling temperature *TfreeCool* to the virtual slab node representing the plane at which the distribution system (TABS or cooled ceiling) is located (cf. Fig. 3 and Eq. (8)):

$$\dot{q} = \frac{1}{R_{fc}} \cdot (T_{slab} - TfreeCool) = \frac{\dot{m}_{sp,p} c_p}{(\dot{m}_p c_p)/(\dot{m}_{ct} c_{ct})(1/\varepsilon_{ct} - 1) + (1/\varepsilon_p - 1) + R_t \dot{m}_{sp,p} c_p} \cdot (T_{slab} - TfreeCool) \tag{8}$$

where

$R_t, \dot{m}_{sp,p}, c_p$ System characteristic, mass flow rate and fluid specific heat capacity of the slab piping system
$\varepsilon_p, \dot{m}_p$ Efficiency and mass flow rate of the heat exchanger for system separation between cooling tower and piping system
$\varepsilon_{ct}, \dot{m}_{ct}, c_{ct}$ System characteristics, mass flow rate and fluid specific heat capacity of the wet cooling tower

Table 3
Error analysis of free cooling operation for a number of simulation cases. S2/S5: building system type, see Table 2; pa/sa: building standard is 'Passive house'/'Swiss average'; l/h: construction type is light/heavy; SMA/LUG/MSM: building site is Zurich/Lugano/Marseille.

| Experiment ID site	S2 sa l SMA	S2 pa l LUG	S5 sa l SMA	S5 sa h LUG	S5 pa l MSM	S5 pa h MSM
Max. hourly capacity error	+13%	+25%	+15%	+10%	+26%	+26%
Min. hourly capacity error	−10%	−13%	−7%	−11%	−12%	−13%
Mean error of transferred energy	+1%	+1%	+2%	+1%	+4%	+5%
Yearly no. of free cooling hours	142 h	566 h	168 h	185 h	1185 h	859 h
Part load operation time	20%	15%	10%	6%	6%	4%

Correct dimensioning of the free cooling system is quite decisive for its energy efficiency and controllability. In practice a broad variety of layouts and variants are found, representing different system concepts and component layouts. To restrict the overall number of model variants we chose one layout per distribution system. The chosen "typical" values were $R_{fc3} = 0.33$ [m² K/W] for TABS and $R_{fc5} = 0.29$ [m² K/W] for the cooling ceiling.

As the distribution side (slab piping system) is typically operated in an on/off-mode, the corresponding parameters are constant and equal to the dimensioning values and therefore bear no uncertainties. Another situation is found on the cold generation side. As can be seen from Fig. 12 the recooling efficiency ε_s of the cooling tower is a nonlinear function of the free cooling temperature. For use in the RC model, this system characteristic had to be approximated by a linear function. Whereas the errors of this linearization are small within a large region around the design point of the cooling tower, the power output of the system is over- or underestimated when operated under conditions far away from the design point (e.g. at low wet bulb temperatures). In addition, the part load efficiency was also simplified by assuming that it linearly decreases with the part load scaling factor *fcUsgFact*.

To estimate the impact of these approximations, an error analysis for a number of representative simulation cases was performed (Table 3). Concerning the linearization of the cooling efficiency it was found that even if the hourly capacities exhibit errors in the range of −13% up to +26%, the error in the overall transferred energy is much smaller and therefore uncritical (max. 5%). Part load operation was found to occur only during a small fraction of the time and so it was concluded that the errors due to the neglect of the part load efficiency are negligible as well.

In summary, the chosen modeling approach considers the most important factors, and, albeit mathematically simple, allows the overall behavior of a free cooling system to be accurately represented.
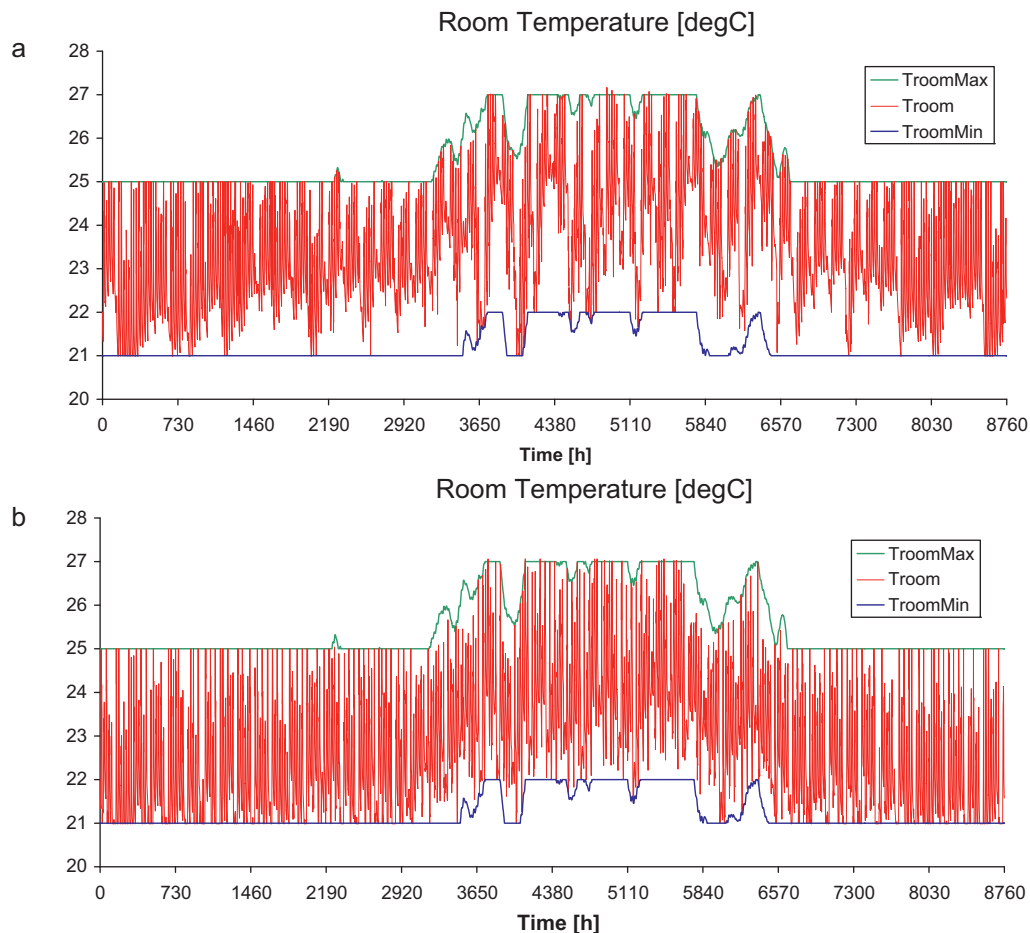
Fig. 13. Yearly room temperature profiles. Left: State-of-the-art Rule-Based Control; Right: Performance Bound simulation (perfect Model Predictive Control). The thermal comfort band width is a function of the 24 h running mean of the outside air temperature and was calculated in a similar manner as described in EN 15251 [15].

4.8. Radiator heating, floor and slab heating and cooling

The radiator heating system was modeled as a direct power input (*hPowRad*) to the room node ϑ_r. Typical radiator devices dissipate approximately 35% and 65% of heat by convection and radiation, respectively. The direct heat transfer to the room node was motivated by the overall approach of using a combined heat transfer coefficient for both, convection and radiation in the model.

Given our focus on the modeling of a single room or building zone we did not model the distribution system and neglected the dissipation of system losses within the building. Further we assumed appropriate system dimensioning, i.e. we assumed that the required heating power (and supply water temperature) can always be provided by the system. These assumptions were also consistent with our approach of providing the radiator heat flux directly into the room node.

The same arguments hold to justify the direct power input to the room node in the case of floor and slab heating and cooling.

4.9. Room illuminance

The room illuminance was modeled to depend on both, available daylight and artificial (electrical) lighting (Eq. (9)). With regard to visual comfort we applied a standard lower illuminance setpoint value for occupied offices of *Eroom,sp* = 500 *lx*. No upper limit was defined, assuming that in case of excess incoming solar radiation the user would be able to obtain glare protection by manual adjustment of an internal blind.

$$E_{room} = E_{dl} + E_{el} = Illum + bPos \cdot dIllum + \eta_{r,el} \cdot etaEl \cdot eLighting \quad (9)$$

The daylight contribution to the room illuminance was calculated according to a correlation used in standard [19]. As can be seen from Eq. (10) the illuminance was computed in function of different parameters of the room and the used glazing. The utilance $\eta_{r,dl}$ summarizes the effects of the room's geometrical and optical properties as well as the light distribution characteristics of diffuse incoming daylight. *etaDl* is the luminous efficacy of solar radiation *RG*. The visual transmission factors of glazing and blind were used to determine the fraction of light which is transmitted to the room. In analogy to the modeling of heat gains through windows illuminance was the sum of a base illuminance with fully closed blinds (*illum*) and an additional part with fully opened blinds (*illum*) which was scaled based on the current blind position.

$$illum = \eta_{r,dl} \cdot etaDl \cdot \tau_{vis,gl} \cdot \tau_{vis,bl0} \cdot \sum_{N,E,S,W} A_{gl,i} \cdot RG_i / A_{floor}$$

$$dIllum = \eta_{r,dl} \cdot etaDl \cdot \tau_{vis,gl} \cdot (1 - \tau_{vis,bl0}) \cdot \sum_{N,E,S,W} A_{gl,i} \cdot RG_i / A_{floor} \quad (10)$$

Illumination by electrical lighting was assumed to vary linearly with the used electrical power. We assumed an ideal electrical lighting control with continuous adjustment depending on the availability of daylight such that the lower illuminance set point was respected at all times. This corresponds to a modern constant illuminance control using dimmers.

5. Example

In this section the application of the developed model is illustrated for one specific case representative of many newly constructed office buildings: a "passive house" building with building system variant S2, façade orientation "South", construction type "lightweight", a "high" window area fraction, internal gains level "high" and indoor-air quality controlled ventilation (case

SMA_S2_pa_S_l_wh_ih_W). The building was assumed to be located at site "Zurich" and the weather data used were given by an average design reference year.

Fig. 13 shows a comparison of two simulated yearly room temperature profiles. The curve on the left represents the results obtained by applying an advanced, state-of-the-art rule based control strategy (RBC-3, Chapter 3 in [20]). The results on the right stem from a simulation using model predictive control (MPC) with a prediction horizon of 6 days and perfect knowledge of the building characteristics and perfect forecast of occupancy and weather boundary conditions (PB, performance bound simulation).

Distinct differences between the two variants can be observed: whereas with RBC the comfort range is regularly fully exploited, with MPC the daily room temperature amplitudes are often smaller. With a non-renewable primary energy demand (NRPE) of 29.3 kWh/(m^2 a) for RBC and 24.6 kWh/(m^2 a) for PB, there is a theoretical NRPE savings potential of 4.7 kWh/(m^2 a) or 16% when using MPC.

In the following paragraphs we highlight the mechanisms that contributed to the found NRPE savings potential based on a selected subset of the hourly simulation results, a 16-day window during February (Fig. 14).

The top panel summarizes the outdoor meteorological conditions (RGS: global solar radiation component on south facing wall) and the room's occupancy status (office working hours), while the remaining panels juxtapose the simulation results obtained from the MPC calculation (bold/blue) with those from the RBC simulation (light/orange). The second panel of Fig. 14 compares the simulated room temperatures (Troom). It can be seen that the MPC-simulated temperatures were mostly above those from the RBC simulation. In particular, the simulated temperatures under the RBC control often was at the lower bound of the thermal comfort range (21 °C), while the MPC temperatures floated within it most of the time.

In order to guarantee thermal comfort the RBC controller repeatedly employed radiator heating (hPowRad, fourth panel), for instance during February 17th and into the morning of February 18th, a period during which outside air temperatures (Tair, top panel) coincided with very low radiation input (RGS) and low internal gains due to the room not being occupied (occup). In contrast to this behavior, the MPC simulation used most of the time no radiator heating at all.

The main reason was due to differences in blind operation (bPos, third panel, 0 = blinds closed): MPC kept the blinds much more open than the RBC algorithm, thus making better use of the incident radiation for (pre-)heating of the room. Quite differently, RBC aimed at reducing heating power by stronger use of energy recovery as compared to MPC (ercUsgFact, last panel).

A further consequence of the optimal blind control by MPC was the avoidance of situations where energy was required for cooling. E.g. it can be seen that during the night of February 13th to 14th MPC kept the blinds open in order to pre-cool the room in anticipation of the solar (RGS) and internal gains (occup) that were expected for the next day. The pre-cooling was also supported by the shown reduction in the energy recovery usage factor (ercUsgFact, 0 = energy recovery deactivated) that resulted into a lower inlet air temperature. In contrast, the RBC strategy managed to keep the room temperature below the upper comfort limit of 25 °C only with the aid of occasional free cooling pulses (fcUsgFact, second bottom panel, 0 = free cooling deactivated), as this was e.g. the case during the afternoon of February 14th.

Readers interested in additional simulation cases or issues concerning the used control algorithms, will find comprehensive analyses and descriptions in [20].
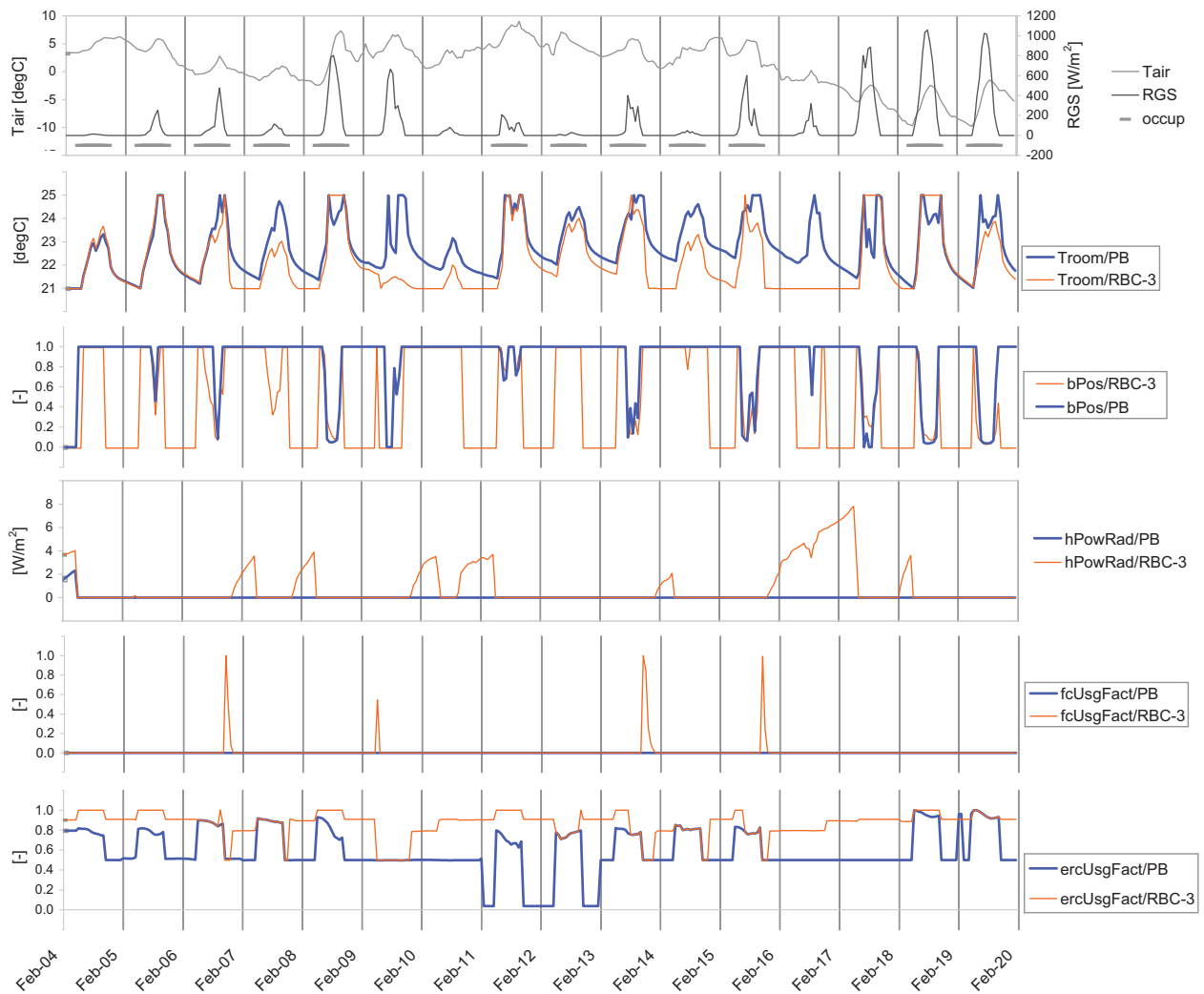
Fig. 14. Comparison of hourly results from the Performance Bound simulation (PB, perfect Model Predictive Control) and the simulation using Rule–Based Control (RBC-3).

6. Concluding remarks

To our knowledge the proposed model – although based on the widespread thermal resistance-capacitance (RC) modeling approach – is quite unique. This is due to its generality, flexibility, and in particular due to its suitability for Model Predictive Control (MPC) that ultimately enables the calculation of a given system's energetic Performance Bound (PB). Other works mostly focus either on a particular building or on a specific building system, and are often not suited for MPC.

Also, the model fills a gap in terms of sophistication and detail between existing, simpler RC models and detailed building physics simulation software. The model enables simulations with a high temporal resolution of 1 h or less, and is computationally efficient. For example an annual PB calculation and a year long simulation using rule-based control on a modern desktop computer take ca. 10 min and ca. 1 min, respectively.

Thanks to a relatively detailed modeling of the thermal masses such as walls and slabs the model yields a very realistic representation of thermal room dynamics. Comparisons with the TRNSYS building simulation software suggest an accuracy in the simulation of hourly mean room temperatures in the order of ±0.5 K. The

derived simplified HVAC equipment models also yield satisfactory results.

The model was developed with the Integrated Room Automation (IRA) in mind. Accordingly, its main limitation is that it focuses on a single room, thus neglecting thermal couplings between neighboring zones. Its extension to several zones appears however straight-forward. The integration of additional building systems might require additional effort in order to cast them into the needed (bi)linear framework. However, note that the model already supports many commonly used systems.

One important field of application are large scale simulation studies, for example for PB analyses of different building and technical system variants in terms of energy consumption and thermal comfort, for systematic parameter sensitivity studies, or for the performance assessment of control strategies using the PB as a benchmark.

The availability of a suitable dynamical model presents a first, important step toward the integration of MPC into Building Automation and Control software and related products. Further steps relate to the identification of the model parameters for a given target building, the estimation of system states to be used as a feed back to the MPC controller, and the interplay of MPC with field level control. These topics will be addressed in future research.

Acknowledgements

References

[1] Schweizerische Gesamtenergiestatistik 2009, Swiss Federal Office of Energy SFOE, Berne, Switzerland, 2010.
[2] EnergyPlus 6.0.0, Energy simulation software, U.S. Department of Energy, SW Washington USA, 2010.
[3] ESP-r 11.10, Integrated energy modeling and simulation program, ESRU, University of Strathclyde, UK, 2010.
[4] IDA ICE 4.0, IDA Indoor Climate and Energy, Equa Simulation AB, Solna, Sweden.
[5] TRNSYS 16.1, Transient system simulation program, SEL, University of Wisconsin USA, TRANSSOLAR, Stuttgart, Germany, 2006.
[6] Standard EN 13790:2009, Energy performance of buildings – calculation of energy use for space heating and cooling.
[7] J. Wen, T.F. Smith, Development and validation of online models with parameter estimation for a building zone with VAV system, Energy and Buildings 39 (2007) 13–22.
[8] A. Mahdavi, C. Pröglhöf, A model-based approach to natural ventilation, Building and Environment 43 (2008) 620–627.
[9] H. Karlsson, E.C. Hagentoft, Application of model based predictive control for water-based floor heating in low energy residential buildings, Building and Environment 46 (2011) 556–569.
[10] M. Kummert, P. André, Simulation of a model-based optimal controller for heating systems under realistic hypothesis, in: Proceedings of the 9th International Building Performance Simulation Association (IBPSA) Conference, Montréal, Canada, 2005.
[11] Y. Yan, et al., Adaptive optimal control model for building cooling and heating sources, Energy and Buildings 40 (2008) 1394–1401.
[12] Y. Ma, et al., Model Predictive Control of thermal energy storage in building cooling systems, in: Proceedings 48th IEEE Conference on Decision and Control and 28th Chinese Control Conference, Shanghai, 16–18 December, 2009, pp. 392–397.
[13] G.P. Henze, C. Felsmann, G. Knabe, Evaluation of optimal control for active and passive building thermal storage, International Journal of Thermal Sciences 43 (2004) 173–183.
[14] R.Z. Freire, G.H.C. Oliveira, N. Mendes, Predictive controllers for thermal comfort optimization and energy savings, Energy Buildings 40 (2008) 1353–1365.
[15] Standard EN 15251:2007, Eingangsparameter für das Raumklima zur Auslegung und Bewertung der Energieeffizienz von Gebäuden – Raumluftqualität, Temperatur, Licht und Akustik.
[16] Technical bulletin SIA Merkblatt 2023, Lüftung in Wohnbauten, Anhang C (Fensterlüftung), SIA, Swiss Society of Engineers and Architects, Zurich Switzerland, 2004.
[17] M. Koschenz, B. Lehmann, Thermoaktive Bauteilsysteme TABS, ISBN 3-905594-19-6 [in German], Empa Duebendorf Switzerland, 2000.
[18] M. Gwerder, B. Lehman, J. Tödtli, V. Dorer, F. Renggli, Control of thermally activated building systems TABS, Applied Energy 85 (2008) 565–581.
[19] Technical bulletin SIA Merkblatt 2044, Klimatisierte Gebäude – Standard-Berechnungsverfahren für den Leistungs-und Energiebedarf, SIA, Swiss Society of Engineers and Architects, Zurich, Switzerland, 2010.
[20] D. Gyalistras, M. Gwerder (Eds.), Use of Weather and Occupancy Forecasts for Optimal Building Climate Control (OptiControl): Two Years Progress Report, Terrestrial Systems Ecology ETH Zurich, Switzerland and Building Technologies Division, Siemens Switzerland Ltd., Zug, Switzerland, 2010, Available from: http://www.opticontrol.ethz.ch (last accessed December 2012).